Spectroscopy of ^{99}Cd and ^{101}In from β decays of ^{99}In and ^{101}Sn

J. Park,[1,2,*] R. Krücken,[1,2] A. Blazhev,[3] D. Lubos,[4,5,6] R. Gernhäuser,[4] M. Lewitowicz,[7] S. Nishimura,[5] D. S. Ahn,[5] H. Baba,[5] B. Blank,[8] P. Boutachkov,[9] F. Browne,[5,10] I. Čeliković,[7,11] G. de France,[7] P. Doornenbal,[5] T. Faestermann,[4,6] Y. Fang,[12] N. Fukuda,[5] J. Giovinazzo,[8] N. Goel,[9] M. Górska,[9] H. Grawe,[9] S. Ilieva,[13] N. Inabe,[5] T. Isobe,[5] A. Jungclaus,[14] D. Kameda,[5] G. D. Kim,[15] Y.-K. Kim,[15,16] I. Kojouharov,[9] T. Kubo,[5] N. Kurz,[9] Y. K. Kwon,[15] G. Lorusso,[5] K. Moschner,[3] D. Murai,[5] I. Nishizuka,[17] Z. Patel,[5,18] M. M. Rajabali,[1] S. Rice,[5,18] H. Sakurai,[5,19] H. Schaffner,[9] Y. Shimizu,[5] L. Sinclair,[5,20] P.-A. Söderström,[5] K. Steiger,[4] T. Sumikama,[17] H. Suzuki,[5] H. Takeda,[5] Z. Wang,[1] H. Watanabe,[21] J. Wu,[5,22] and Z. Y. Xu[19]

[1] *TRIUMF, 4004 Wesbrook Mall, Vancouver, British Columbia V6T 2A3, Canada*
[2] *Department of Physics and Astronomy, University of British Columbia, Vancouver, British Columbia V6T 1Z1, Canada*
[3] *Institute of Nuclear Physics, University of Cologne, D-50937 Cologne, Germany*
[4] *Physik Department, Technische Universität München, D-85748 Garching, Germany*
[5] *RIKEN Nishina Center, Wako-shi, Saitama 351-0198, Japan*
[6] *Excellence Cluster Universe, Technische Universität München, D-85748 Garching, Germany*
[7] *Grand Accélérateur National d'Ions Lourds (GANIL), CEA/DSM-CNRS/IN2P3, Boulevard H. Becquerel, 14076 Caen, France*
[8] *Centre d'Etudes Nucléaires de Bordeaux-Gradignan, 19 Chemin du Solarium, CS 10120, F-33175 Gradignan Cedex, France*
[9] *GSI Helmholtzzentrum für Schwerionenforschung GmbH, D-64291 Darmstadt, Germany*
[10] *School of Computing, Engineering and Mathematics, University of Brighton, Brighton BN2 4GJ, United Kingdom*
[11] *Vinča Institue of Nuclear Sciences, University of Belgrade, 11000 Belgrade, Serbia*
[12] *Osaka University, Machikaneyama-machi 1-1, Toyonaka, Osaka 560-0043, Japan*
[13] *Technische Universität Darmstadt, D-64289 Darmstadt, Germany*
[14] *Instituto de Estructura de la Materia, IEM-CSIC, E-28006 Madrid, Spain*
[15] *Rare Isotope Science Project, Institute for Basic Science, Daejeon 305-811, Republic of Korea*
[16] *Department of Nuclear Engineering, Hanyang University, Seoul 133-791, Republic of Korea*
[17] *Department of Physics, Faculty of Science, Tohoku University, Sendai 980-0845, Japan*
[18] *Department of Physics, University of Surrey, Guildford GU2 7XH, United Kingdom*
[19] *University of Tokyo, 7-3-1 Hongo Bunkyo, Tokyo 113-0033, Japan*
[20] *University of York, York YO10 5DD, United Kingdom*
[21] *Beihang University, Beijing 100191, China*
[22] *Department of Physics, Peking University, Beijing 100871, China*

(Received 27 April 2020; accepted 17 June 2020; published 6 July 2020)

We report on new γ-ray spectroscopy results from β decays of ^{99}In and ^{101}Sn. 30 new γ rays were observed following the β decay of ^{99}In, and inconsistencies in the literature with respect to the γ rays following the β decay of ^{101}Sn were addressed with two confirmed cases and two new transitions. The experimental γ-ray energies, intensities, and coincidence relationships are discussed with shell model calculations, where theoretical β-decay branching ratios from the parent nuclei and γ-ray cascades of excited states from the daughter nuclei were combined to generate hypothetical $\beta\gamma$ spectra and $\beta\gamma\gamma$ coincidence matrices. The most intense β-delayed γ-ray branches in both ^{99}Cd and ^{101}In were well reproduced with this approach, and several γ rays were assigned to new excited states based on their good agreement with shell model predictions.

DOI: 10.1103/PhysRevC.102.014304

I. INTRODUCTION

Atomic nuclei far away from stability feature many interesting structure phenomena, and one of them is the evolution of nuclear shells through the changes in effective single-particle energies (ESPE) [1–4]. In particular, the monopole part of the tensor force originating from the π and $\pi+\rho$ meson exchange processes between proton and neutron orbits was shown to be essential to describe the ESPE trends near shell closures [5,6]. A strong tensor force is expected to manifest in the ESPE of nuclei around the doubly magic ^{100}Sn due to the interaction between the proton (π) $g_{9/2}$ orbital below $Z=50$ and the neutron (ν) $g_{7/2}$ orbital above the $N=50$ shell. As the $\pi g_{9/2}$ orbital is filled, a trend of decreasing ESPE of the $\nu g_{7/2}$ orbital relative to the $\nu d_{5/2}$ orbital has been observed experimentally in even Z, $N=51$ isotones [7]. The excitation energy (E_x) of the yrast ($7/2^+$)

*Present address: Center for Exotic Nuclear Studies, Institute for Basic Science (IBS), Daejeon 34126, Republic of Korea; jcpark@ibs.re.kr

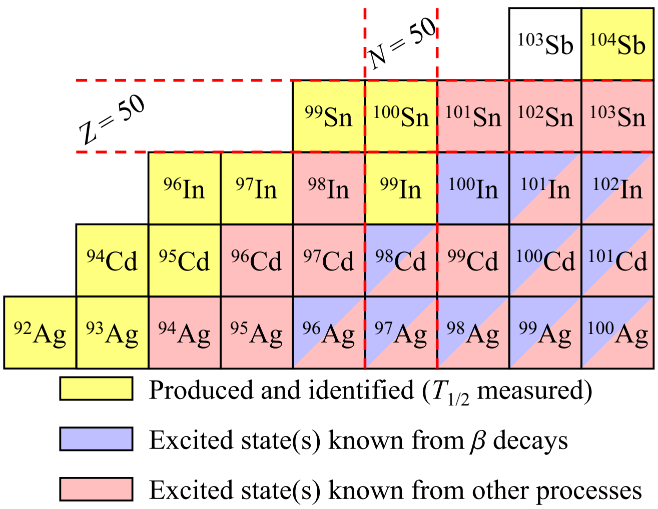

FIG. 1. Segrè chart of nuclides around the doubly magic nucleus ^{100}Sn. Different colors indicate the available experimental information for each nucleus. The amount of knowledge on excited state(s) varies widely among the different nuclei.

state in ^{99}Cd has been found to be 441 keV above the $(5/2^+)$ ground state [8], supplementing the first spectroscopy results for this nucleus [9]. On the other hand, the energy gap of the two states in ^{101}Sn was first measured to be 172 keV [10] but without a clear consensus on the order of the two spins for ^{101}Sn [11–13]. The order and the energy splitting of the two nearly degenerate states in this nucleus have received theoretical treatments involving three-nucleon forces [14].

Excited states of proton-rich nuclei in the ^{100}Sn region have been studied via fusion-evaporation experiments involving $A \approx 50$ beams and target nuclei [15]. This method had an advantage of the residual nuclei being populated in high-spin and high-energy states, revealing many γ rays and core excitations to be compared with shell model (SM) calculations. Advancements in rare isotope production capabilities with heavy-ion fragmentation enabled supplementary isomer and β-decay γ-ray spectroscopy of the same isotopes, allowing investigations of their low-energy and low-spin structures. The current status of the published experimental knowledge of nuclei in the vicinity of ^{100}Sn is shown in Fig. 1. It should be noted that the depth of knowledge of excited states ranges from mere evidence of a long-lived isomer or unassigned γ-ray transitions to a detailed level scheme with $\gamma\gamma$ coincidence relations and measured electromagnetic transition strengths. The level scheme of ^{99}Cd has not yet been revealed through β-delayed γ-ray spectroscopy. For ^{101}In, γ rays which have been detected after the β decay of ^{101}Sn were few in number and inconsistent among previous experiments [11,16]. In order to enhance the understanding of the structure of the two nuclei in the context of $N \approx Z$ systems near ^{100}Sn, we present and discuss new γ-ray spectroscopy results on ^{99}Cd and ^{101}In from β decays of ^{99}In and ^{101}Sn.

II. EXPERIMENT AND ANALYSIS

The decay spectroscopy experiment was carried out at the Radioactive Isotope Beam Factory of RIKEN Nishina Center. ^{99}In, ^{101}Sn, and other proton-rich $N \leqslant 51$, $Z \leqslant 50$ nuclei were produced by fragmentation reactions of a 345-MeV/u ^{124}Xe beam on a 740-mg/cm^2 Be target. Isotope separation and identification of the radioactive ions were achieved through the BigRIPS separator and the ZeroDegree spectrometer [17,18]. The ions were implanted in one of the three double-sided silicon strip detectors (DSSSDs) of the WAS3ABi detector [19], where each DSSSD was 1 mm thick and featured 60/40 1-mm-wide strips for x-y position measurements, respectively. All β-decay or β-delayed proton (βp) emission events within one-pixel distance from the ion implantation event were correlated. A stack of ten single-sided silicon strip detectors was placed behind the DSSSDs for positron calorimetry. The decay events were correlated with the implanted nuclei in WAS3ABi according to spatial and timestamp matching schemes. γ rays emitted either from isomeric states which were populated during fragmentation, or after $\beta/\beta p$ decays, were detected with the high-purity germanium Euroball-RIKEN Cluster Array (EURICA) [20]. For this experiment, EURICA was operated at 4.6% detection efficiency for γ rays at 1 MeV with energy addback. More details of the experimental and analysis methods are provided in Refs. [21–24].

III. RESULTS

Approximately 2×10^5 ^{99}In and 9×10^3 ^{101}Sn ions were produced, identified, and implanted in WAS3ABi for decay spectroscopy. The implantation-to-β-decay correlation efficiencies of the two nuclei were 70(1)% and 69(2)%, respectively. The β-decay half-lives ($T_{1/2}$) and β-delayed proton emission branching ratios ($b_{\beta p}$) of ^{99}In and ^{101}Sn were determined as 3.11(6) s/0.29(3)% and 2.22(5) s/23.6(8)%, respectively [23]. With the exception of $b_{\beta p}(^{101}\mathrm{Sn})$, these values are more precise than those listed in the latest NUBASE2016 database [25]. Evidence of isomeric states in the two nuclei and their β-decay daughters was not found in this experiment.

A. γ rays in ^{99}Cd from the β decay of ^{99}In

The γ-ray spectrum obtained from correlated β decay events of ^{99}In is shown in Fig. 2, where the β-decay correlation time window was 0–5 s after ion implantation. A negative time correlation window was used to generate a randomly correlated $\beta\gamma$ spectrum, which was used in the background subtraction. Transitions with energies 156, 226, 441, 607, 784, 1224, and 1234 keV, previously assigned to ^{99}Cd [8], were also measured in this work. Twenty-nine new γ rays with γ-gated β-decay $T_{1/2}$ consistent with the measured $T_{1/2}$ of ^{99}In within 2σ were observed, ranging in energy from 100 to 5000 keV. In addition, one γ ray was observed at 481 keV with a β-decay $T_{1/2}$ of 4.82(73) s, 2.3σ greater than the overall value of 3.11(6) s. The absence of $\gamma\gamma$ coincidences hindered an unambiguous assignment of this γ ray to a particular nucleus. Even though γ rays with matching energies were reported in several nuclei other than ^{99}Cd, their most intense γ rays were not observed in the $\beta\gamma$ spectrum. Therefore, the 481-keV γ ray was tentatively assigned to an unknown excited state in ^{99}Cd populated by the β decay of ^{99}In. The intensities of all

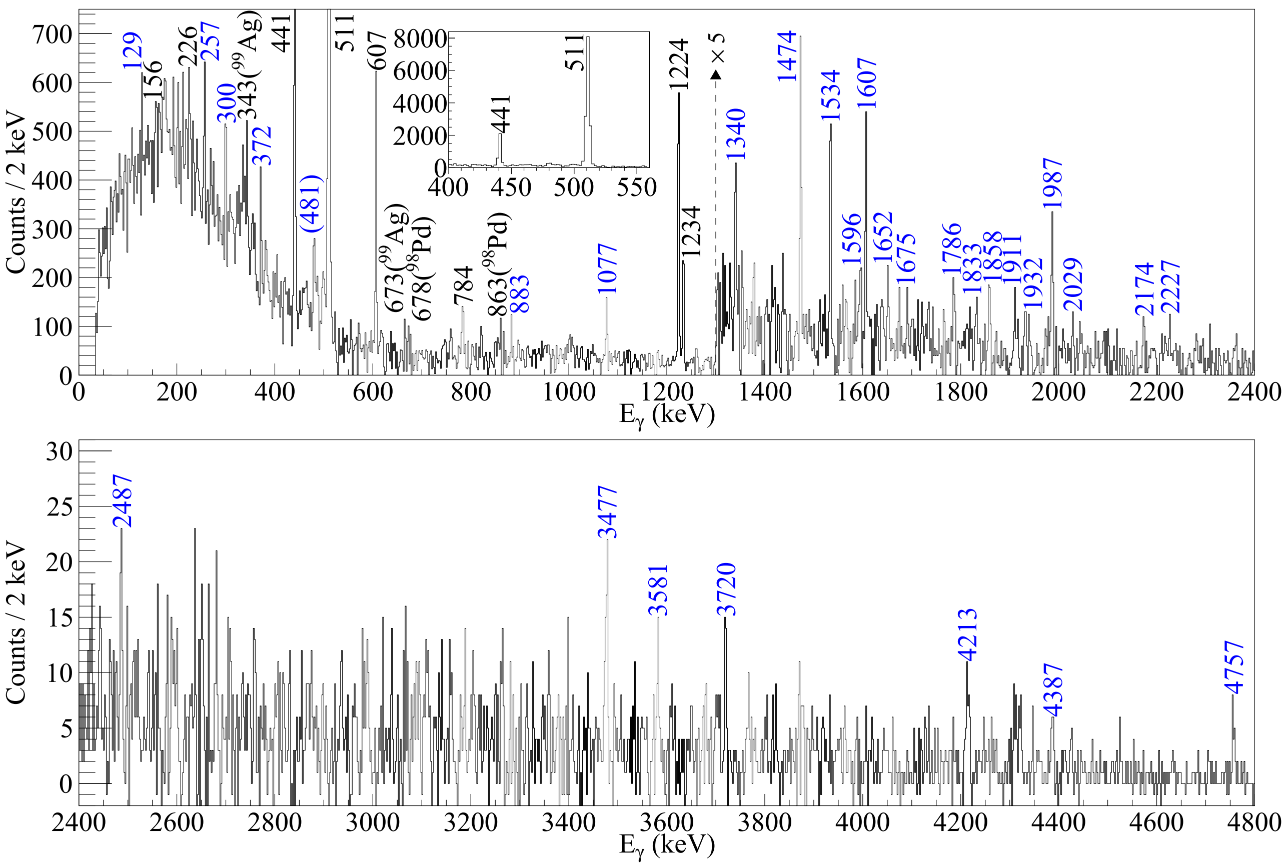

FIG. 2. Background-subtracted γ-ray spectra of β-decay events correlated between 0 and 5 s after ^{99}In implantation. The peaks labeled in black correspond to the previously observed γ rays in ^{99}Cd [8] and other background contaminants as labeled. New transitions from this decay spectroscopy experiment are labeled in blue. See the text for the tentative assignment of the 481-keV γ ray in ^{99}Cd. The full amplitudes of the 441-keV γ-ray line and the 511-keV electron-positron annihilation peak are shown in the inset.

of the γ rays assigned to ^{99}Cd from the β decay of ^{99}In are listed in Table I.

The $\gamma\gamma$ coincidence projections of some of the most intense transitions are shown in Fig. 3. Some of the low-energy γ-ray coincidences are tentative. The low-spin level scheme of ^{99}Cd was confirmed based on the coincidence relations between the 441-, 607-, and 1224-keV γ rays. Five new $\gamma\gamma$ coincidences with the $(7/2_1^+) \rightarrow (5/2_1^+)$ 441-keV transition were observed at 1340, 1534, 1786, 1987, and 2487 keV. On the other hand, the 1224-keV γ ray corresponding to the $(9/2_1^+) \rightarrow (5/2_1^+)$ transition was coincident with the 257-, 1474-, and 1596-keV γ rays. The 1474-keV γ ray was also coincident with the 607-keV $(13/2_1^+) \rightarrow (9/2_1^+)$ γ ray, which suggests a new excited state with $E_x \geqslant 3305$ keV. Despite sufficient statistics in the γ-ray singles spectrum, the absence of $\gamma\gamma$ coincidences for the 883-, 1077-, and 1607-keV γ rays suggest new excited states in ^{99}Cd at those energies. Additional $\gamma\gamma$ coincidence relationships with the newly observed γ rays could not be established due to either a lack of statistics or low peak-to-background ratios. The proposed level scheme of ^{99}Cd is shown in Fig. 4, and the placement of some of the new γ rays is discussed in Sec. IV A.

B. γ rays in ^{101}In from the β decay of ^{101}Sn

The γ-ray spectrum following β decays of ^{101}Sn is shown in Fig. 5, generated with a β-decay correlation time window of 0–3 s. The same background subtraction method was applied as in the case of ^{99}In $\beta\gamma$ spectroscopy. Two of the γ rays observed in Ref. [16], with 1346 and 1500 keV, were also seen in this experiment. In addition to the confirmed transitions, two new γ rays with 2116 and 2157 keV were observed. The β-decay time distributions obtained from the γ-ray gates on the four observed transitions resulted in consistent $T_{1/2}$ values with the overall half-life of ^{101}Sn. On the other hand, no evidence was found for the 352- and 1065-keV γ rays which were reported in Ref. [11]. Furthermore, the 252, 1281-, 1333-, and 1508-keV γ rays which were reported in Ref. [16] were not observed with statistical significance in this experiment. A small peak near 1281 keV has a centroid of 1284 keV, whose energy difference is more than 2σ in terms of the EURICA resolution. The 252-keV transition had been associated with the decay of the first-excited state in the granddaughter nucleus ^{101}Cd [27], but was perhaps incorrectly assigned to the β decay of ^{101}Sn in Ref. [16]. The intensities of the γ rays measured in this work are given in Table II. The lack of statistics prevented $\gamma\gamma$ coincidence analyses for this data set.

TABLE I. Energies and intensities of γ-ray transitions marked in Fig. 2 following the β decay of ^{99}In, where I_γ were normalized to the number of observed ^{99}In β decays. I_γ^{rel} values refer to the γ-ray intensities which were normalized to the I_γ value of the 441-keV γ ray. Only the intensities of transitions with $E_\gamma \leqslant 300$ keV were corrected for internal conversion based on Ref. [26], assuming pure $M1$ multipolarity due to their prompt decay times.

E_γ (keV)	I_γ (%)	I_γ^{rel} (%)
129.3(5)	3.3(17)	7.7(39)
156.5(4)	2.2(15)	5.2(35)
225.9(2)	5.9(15)	14.0(35)
257.3(2)	4.6(14)	10.8(32)
300.0(3)	4.6(15)	10.7(34)
371.6(3)	5.2(11)	12.4(26)
440.8(1)	42.3(15)	100.0(34)
480.6(3)	5.0(12)	11.8(27)
606.9(1)	13.4(10)	31.6(23)
783.8(4)	4.3(9)	10.3(20)
882.9(2)	3.3(8)	7.7(18)
1076.7(2)	5.2(9)	12.3(21)
1224.2(1)	28.0(12)	66.2(29)
1234.0(1)	11.3(9)	26.8(21)
1340.4(3)	4.3(8)	10.2(18)
1473.6(2)	6.2(8)	14.7(18)
1534.1(2)	5.8(8)	13.6(19)
1596.2(4)	2.1(7)	4.9(17)
1606.6(2)	4.3(7)	10.2(16)
1652.0(4)	1.8(7)	4.3(16)
1675.0(4)	2.1(7)	3.4(14)
1785.8(3)	3.5(6)	8.3(14)
1832.6(6)	1.7(6)	4.0(12)
1858.4(5)	2.7(6)	6.4(14)
1911.0(6)	2.1(6)	4.9(12)
1931.8(6)	2.1(6)	5.1(13)
1987.1(3)	4.1(6)	9.6(15)
2029.0(6)	0.9(5)	2.1(12)
2173.7(5)	1.2(5)	2.7(12)
2227.1(6)	1.2(5)	2.9(12)
2486.7(5)	2.3(5)	3.2(12)
3476.9(8)	3.0(6)	7.1(13)
3580.8(7)	2.4(5)	5.7(11)
3719.9(5)	1.6(4)	3.8(10)
4213.4(9)	2.2(4)	5.1(10)
4386.9(8)	1.5(4)	3.4(9)
4756.8(9)	1.6(4)	3.9(9)

IV. DISCUSSION

Being close to the presumably doubly magic ^{100}Sn, ^{99}Cd and ^{101}In serve as good test cases of both empirical and modern SM approaches. Single-particle energies of the nucleons above an assumed inert core of ^{88}Sr and two-body matrix elements (TBME) of their interactions in the proton/neutron model space consisting of proton $2p_{1/2}$ and $1g_{9/2}$ orbitals below the $Z = 50$ shell, and neutron $1g_{7/2}$, $2d_{5/2}$, $2d_{3/2}$, $3s_{1/2}$, and $1h_{11/2}$ orbitals between the $N = 50$ and the $N = 82$ shells have been employed to describe the structure of nuclei with similar N and Z [8,11,28].

For this work, the SM results were derived from the SR88MHJM interaction [11,15,28] through the NuShellX software [29]. As the name of the model suggests, ^{88}Sr ($Z = 38, N = 50$) was taken as the basis for the nuclear core. The model space for this interaction includes the same positive and negative-parity orbitals mentioned in the previous paragraph, but only positive-parity states were calculated here. β-decay branching ratios (b_β) were calculated for allowed GT transitions only, i.e., $|J_f - J_i| \leqslant 1$ with no parity change. When calculating B_{GT} values of ^{99}In and ^{101}Sn using such a phenomenological model, the β-decay coupling must be quenched. A systematic evaluation of the experimental GT β decays of $44 \leqslant Z \leqslant 50$, $50 \leqslant N \leqslant 58$ nuclei proposed a quenching factor $q = 0.56(2)$ for an analogous but different SM [12], but may have a range wider than 0.40–0.65 from the experimentally known B_{GT} values of $N = Z + 2$ nuclei. A quenching factor $q = 0.3$ applied on the results from the SR88MHJM interaction yielded $B_{\mathrm{GT}}^{\mathrm{theo}}(^{99}\mathrm{In}) = 4.8$ and $B_{\mathrm{GT}}^{\mathrm{theo}}(^{101}\mathrm{Sn}) = 4.7$ or 5.3, where the two values correspond to the $7/2^+$ and $5/2^+$ hypotheses on the ground-state spin of ^{101}Sn, respectively. Total absorption spectrometer (TAS) measurements of the decays of the two nuclei for B_{GT} distributions and the summed values are desired. The input Q_{EC} values for the two nuclei were adopted from the Atomic Mass Evaluation 2016 [30] in order to predict decay half-lives in a range of 1.8–3.7 s for ^{99}In and 1.0–5.9 s for ^{101}Sn for $q = 0.3$–0.6. The wider range of $T_{1/2}$ for ^{101}Sn originates from the different shapes of GT distributions depending on the ground-state spin hypothesis. These $T_{1/2}$ values are in a reasonable agreement with the measured values.

As a more microscopic comparison between the experimental and theoretical results, the measured E_γ and I_γ values were compared to their theoretical counterparts. They were calculated based on SM predictions of β-decay energies/intensities, J^π of the predicted states, and effective charges: artificial adjustments of the proton and neutron magnetic g factors and electric charges in order to compensate for core polarization and model space truncation. The dependence on the transition energy and the effective charges on the calculated γ-ray branching ratios was examined. Only the theoretical electromagnetic transitions with $M1$ and/or $E2$ multipolarity components were considered, in order to eliminate discussions of poorly known higher-multipolarity transitions that possess presumably low branching ratios. The effective g factors for the calculation of $B(M1)$ values were set to be $g_s^{\mathrm{eff}} = 0.7 g_s^{\mathrm{free}}$ for both protons and neutrons, in order to reproduce the observed magnetic moments of the yrast $5/2^+$ states in light, odd-mass Cd isotopes [28]. By assuming the ^{88}Sr core, the calculated $B(E2)$ values for the $N = 50$ nucleus ^{98}Cd depend only on the proton effective charge. While the experimental $B(E2)$ value for the $(8_1^+) \rightarrow (6_1^+)$ transition is well reproduced with $e_p = 1.5e$, the $B(E2)$ value for the $(6_1^+) \rightarrow (4_1^+)$ decay agrees better with $e_p = 1.7e$. The effective charge set of $e_p = 1.7e$, $e_n = 1.0e$ has been used for Cd isotopes in Refs. [28,31]. Meanwhile, the literature $B(E2)$ value of the $(6_1^+) \rightarrow (4_1^+)$ transition in ^{102}Sn [16] provides a reference for tuning of the neutron effective charge for the SR88MHJM interaction, whose proton model space is limited to $Z \leqslant 50$.

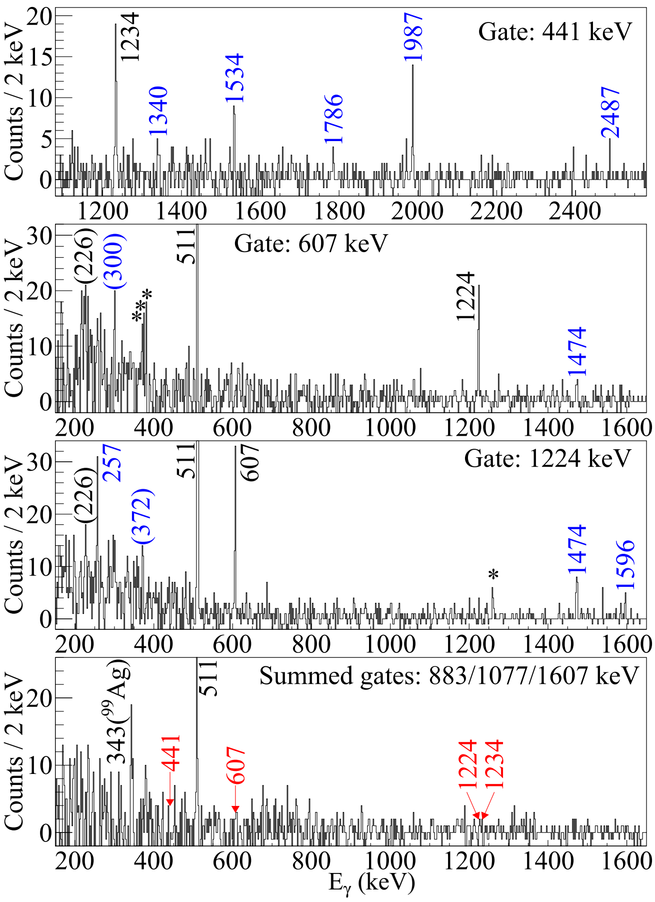

FIG. 3. $\gamma\gamma$ coincidence projections of some of the transitions shown in Fig. 2, with gates as indicated in each histogram. The black and blue color schemes on the energy labels are the same as in Fig. 2, and those with red labels indicate the absence of coincidences with the most intense γ rays in ^{99}Cd. The peaks which are marked with energies in parentheses are tentative coincidences. The transitions marked with asterisks are Compton peaks from random background γ rays originating from much more abundant nuclei, such as ^{97}Pd.

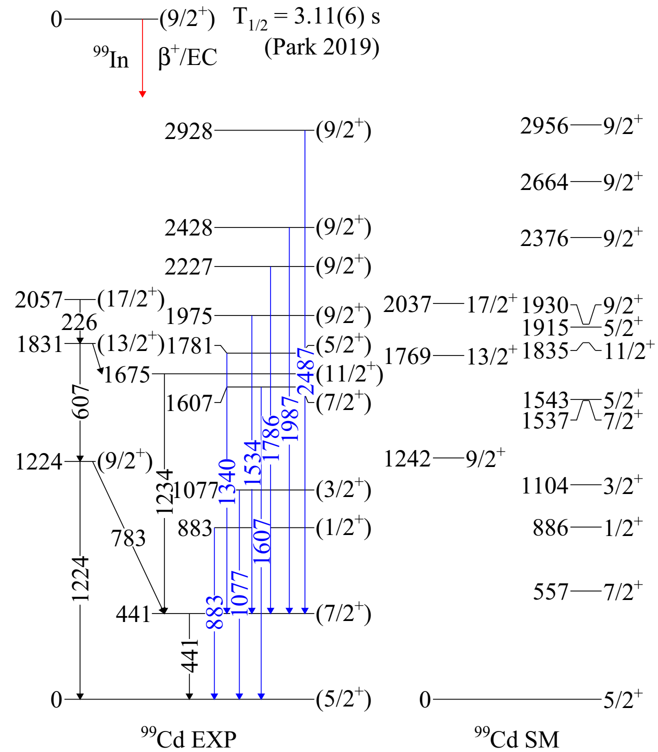

FIG. 4. Level schemes of ^{99}Cd from the $\beta\gamma$ spectroscopy of ^{99}In. The half-life of ^{99}In was determined in a previous work (Park 2019 [23]). The energies of the states and the transitions are in keV. The states which are linked by black arrows were previously assigned in Ref. [8]. New γ rays which were placed in the level scheme of ^{99}Cd are drawn as blue arrows. For the SM results, only the most relevant states for comparison with the proposed experimental level scheme are shown.

As seen in Table III, $e_n = 1.4e$ reproduces the experimental $B(E2)$ value well compared to other e_n values. The results of e_p and e_n tuning for $E2$ transitions in an odd-odd nucleus ^{98}Ag and even-even nucleus ^{100}Cd also support the assumption of $e_p = 1.5e$, $e_n = 1.4e$ for calculations of γ-ray branching ratios in ^{99}Cd and ^{101}In. However, it is noteworthy that the $B(E2)$ value of the $(17/2^+) \rightarrow (13/2^+)$ isomeric transition in ^{99}Cd is better reproduced with $e_p/e_n = 1.5e/0.5e$. Thus this effective charge set, combined with $g_s^{\rm eff} = g_s^{\rm free}$, was also employed to calculate γ-ray intensities in ^{99}Cd.

After combining the β-decay schemes with γ-ray decay cascade schemes from the SM, all of the I_β and I_γ were funneled down to the ground states in the daughter nuclei. The outputs of such exercise were theoretical $\beta\gamma$ spectra and $\beta\gamma\gamma$ matrices, which could then be compared with the available experimental data after efficiency correction. Uncertainties on theoretical β-delayed γ-ray intensities were calculated from multiple sources, but with a common underlying factor: excitation and decay energies. To determine the magnitude of energy discrepancies between theory and experiment, $(E_x^{\rm exp} - E_x^{SM})/E_x^{\rm exp}$ values of 11 experimentally confirmed excited states in ^{99}Cd and ^{101}In [8] were evaluated. The mean and the standard deviation of this distribution were 0.4(4)% and 7(1)%, respectively. The standard deviation was then used for propagating theoretical uncertainties in the following manner. For the states which are fed directly from β decays, the uncertainties on their β-decay intensities were evaluated by shifting their excitation energies up or down by 7% while keeping the $B_{\rm GT}$ values fixed. This perturbation would affect the β-decay phase space integral f and thus provide an uncertainty on the partial half-life t, which was then translated into an uncertainty on I_β. For calculating the uncertainties on the theoretical γ-ray energies, 7% shifts were applied on both the initial and the final states' excitation energies and their uncertainties added in quadrature for setting lower and upper bounds on E_γ. By keeping the electromagnetic transition strengths fixed, the energy uncertainties were converted into uncertainties on the decay rate λ and ultimately the branching ratios by the relation $\lambda_\gamma \propto I_\gamma \propto E_\gamma^{2l+1}$, where l is the transition multipolarity.

A. Comparisons for ^{99}Cd

The projection of experimental and theoretical $\beta\gamma$ intensities for ^{99}Cd is shown in Fig. 6. While some differences in

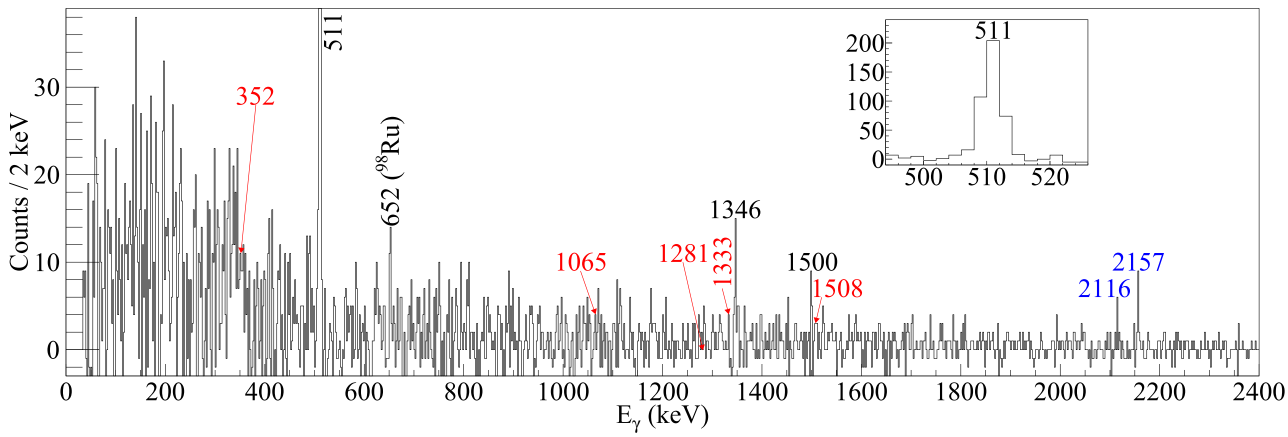

FIG. 5. Background-subtracted γ-ray spectrum of β-decay events correlated between 0 and 3 s after ^{101}Sn implantation. γ-ray energies labeled in black were reported in Ref. [16], and are also observed in this experiment. The energy labels in red accompanied by arrows correspond to the previously reported γ rays [11,16] which were not observed in this work. New transitions assigned to ^{101}In are marked with blue labels. The inset shows the raw intensity of the 511-keV annihilation peak.

the intensities are observed for the different sets of effective charges, their deviations are not significant for many of the transitions. The SM is capable of reproducing the intensities of the four strongest transitions at 441, 607, 1224, and 1234 keV, while overestimating the intensity of the 784-keV transition between the $(9/2_1^+)$ and the $(7/2_1^+)$ states. The effective charge set $e_p/e_n = 1.5/1.4e$ and $g_s^{\rm eff} = 0.7g_s^{\rm free}$ yields I_γ(784 keV) that is closer to the experimental value than the calculated intensity from the effective charge set $e_p/e_n = 1.5/0.5e$ and $g_s^{\rm eff} = g_s^{\rm free}$, albeit with large uncertainties for both because of long γ-decay cascades from high-energy excited states. Note that a reduction of the $(9/2_1^+) \rightarrow (7/2_1^+)$ γ-ray intensity implies an increase of the $(9/2_1^+) \rightarrow (5/2_1^+)$ branching ratio. The large theoretical uncertainties on certain I_γ reflect their sensitivity on the amplitudes of β-decay feeding and/or γ-ray branching ratios. The energy discrepancies of the 441-, 607-, and 784-keV γ rays with the SM results demand some improvements in the calculations. Also, the $11/2_1^+$ state in ^{99}Cd is predicted to be higher in energy compared to the $13/2_1^+$ state, in contrast to the literature which reported a 156-keV γ-ray branch from the $(13/2_1^+)$ state to populate the $11/2_1^+$ state.

The γ-ray peaks at 1340, 1534, 1786, 1987, and 2487 keV in coincidence with the 441-keV transition were not seen in the $\gamma\gamma$ coincidence projection with the 1234-keV γ-ray gate due to low statistics. From these findings, the five previously mentioned γ rays were tentatively placed in the level scheme of ^{99}Cd as parallel branches which feed the 441-keV state, as exhibited in Fig. 4. From the theoretical $\gamma\gamma$ matrix, some of the energies of the intense γ rays (in keV) in coincidence with the equivalent transition of the 441-keV γ ray, and their parent states' J^π values are 1358 from $5/2_3^+$; 1372 from $9/2_2^+$; 1819 from $9/2_3^+$; 2107 from $9/2_4^+$; and 2399 from $9/2_5^+$. The energy values agree within 10.5% of the empirical γ-ray energies, a reasonable range given the 7% 1σ deviation of excitation energies for both the initial and the final states as quoted above. Thus, tentative spins are assigned to the new states, mainly

TABLE II. Energies and intensities of γ-ray transitions assigned to ^{101}In in this work based on Fig. 5, where I_γ were normalized to the number of correlated ^{101}Sn β decays. The I_γ values were not corrected for internal conversion. The γ-ray intensities which were normalized to that of the 1346-keV γ ray are listed under $I_\gamma^{\rm rel}$. Relative intensities from Ref. [16] are listed for comparison.

E_x (keV)	I_γ (%)	$I_\gamma^{\rm rel}$ (%)	$I_{\rm lit}^{\rm rel}$ (%) [16]
1281	<9.7	<38	40(10)
1333	<7.8	<31	50(10)
1346.3(5)	25.2(63)	100(25)	100(20)
1500.2(4)	13.3(47)	53(19)	80(20)
1508	<8.6	<34	20(10)
2116.2(10)	11.4(40)	45(16)	
2157.4(3)	13.4(44)	53(18)	

TABLE III. Experimental $B(E2)$ values from isomers in the vicinity of ^{100}Sn, and the SM values with the SR88MHJM Hamiltonian with different sets of effective charges (e_p/e_n, in units of e). The references for the experimental $B(E2)$ values are given in the footnotes.

Nucleus	$J_i^\pi \rightarrow J_f^\pi$	$B^{\rm exp}(E2)$ (e^2fm^4)	$B^{\rm SM}(E2, e^2{\rm fm}^4)$ 1.5/1.4	1.5/0.5	1.7/1.5
^{98}Ag	$(4_1^+) \rightarrow (6_1^+)$	119(5)[a]	109	46	132
^{98}Cd	$(6_1^+) \rightarrow (4_1^+)$	125(20)[a]	98	98	125
	$(8_1^+) \rightarrow (6_1^+)$	38.5(40)[a]	39.1	39.1	50.2
^{99}Cd	$(17/2_1^+) \rightarrow (13/2_1^+)$	68(3)[b]	95	68	119
^{100}Cd	$(8_1^+) \rightarrow (6_2^+)$	50(22)[c]	77	44	94
	$(8_1^+) \rightarrow (6_1^+)$	0.46(3)[c]	0.41	0.26	0.51
^{102}Sn	$(6_1^+) \rightarrow (4_1^+)$	83(6)[d]	84	11	97

[a]Reference [21].
[b]Reference [9].
[c]Reference [27].
[d]Reference [16].

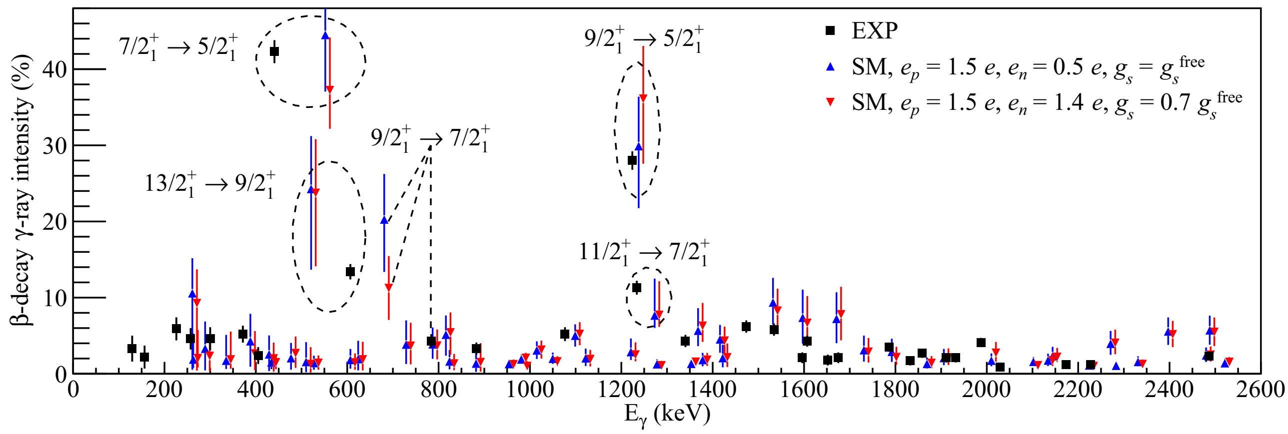

FIG. 6. Experimental (black) and theoretical (blue and red) β-delayed γ-ray intensities in ^{99}Cd. The initial-final spin labels are taken from SM calculations, and the dashed lines and ellipses help guide the reader the matching transitions where tentative spins were previously assigned [8,9].

motivated by the SM results. With the exception of the $5/2^+_3$ state, the non-yrast $9/2^+$ states were predicted to feed the 441-keV ($7/2^+_1$) state with non-negligible intensities. A significant portion of the GT strength of ^{99}In was calculated to lie at $E_x \approx 4400$ keV—far above the $9/2^+_5$ state at $\approx$3000 keV, which implies that higher-multiplicity γ-ray coincidences can confirm or reject the placements of the aforementioned γ rays in the level scheme of ^{99}Cd.

Concerning the 257-, 1474-, and 1596-keV γ rays in coincidence with the 1224-keV transition, theoretical $\gamma\gamma$ coincidence relationships are much more ambiguous and largely inconsistent. The lack of a 257-607 coincidence suggests an excited state at 1481 keV which would feed the 1224-keV ($9/2^+_1$) state, but the only candidate state from the SM which fulfills this role is a $7/2^+_2$ state that has a $78^{+16}_{-14}\%$ branching ratio to the ground state. A strong 1481-keV γ ray was not seen in the experimental data, such that the 257-keV γ ray should be placed much higher in the level scheme with an intermediate transition. A hypothetical 257-1596-1224 cascade, in descending order, is not corroborated by the SM. Likewise, the mutual coincidence of the 1474-keV γ ray with the 607- and 1224-keV γ rays leading to a proposal of a 1474-607-1224 cascade does not have a suitable match in the SM results. Multiple candidate transitions in an energy range of 1350–1700 keV and similar intensities as that of the 1474-keV γ ray are predicted by the SM, and are shown in Fig. 6. However, comparisons between the currently known $\gamma\gamma$ coincidence relationship and the SM-based γ-ray cascades involving these transitions remain largely ambiguous.

The three γ rays at 883, 1077, and 1607 keV without signatures of $\gamma\gamma$ coincidences with the strongest known transitions in ^{99}Cd are energetically well matched with three states which are predicted at 886, 1104, and 1537 keV. These states possess J^π values of $1/2^+$, $3/2^+$, and $7/2^+$ in the ascending order. According to the SM, feeding of these states from above is highly fragmented such that $\gamma\gamma$ coincidence projections are not expected to reveal intense γ rays. These findings provide a basis for the assignment of three new states at 883, 1077, and 1607 keV as shown in Fig. 4. As for the 481-keV γ ray mentioned in Sec. III A, no other spare positive-parity state with $E_x < 1000$ keV in ^{99}Cd was suggested by the SM. The 2.3σ deviation of the γ-gated β-decay half-life associated with this γ ray brings up a possibility of a $1/2^-$ isomer in ^{99}In, but the assignment of this γ ray to ^{99}Cd needs to be firmly established first.

B. Comparisons for ^{101}In

In addition to the propagation of β-decay feeding and γ-ray decay cascades for the SM projection of the $\beta\gamma$ spectrum, an attempt to reproduce the β-delayed proton emission spectrum and its branching ratio was made by partial half-life comparisons between γ-ray and proton emission decay modes from highly excited states in ^{101}In. Given an excited state with energy $E_x > S_p$, protons emitted from that particular state with a kinetic energy $T = E_x - S_p$ and angular momenta $l = 2$ and $l = 4$ from the (g, d) orbitals above the $N = Z = 50$ shells were assigned decay partial half-lives as formulated in Ref. [32] and applied in Refs. [22,33]. The predominance of proton emission with those particular angular momenta was assessed from core-excited states in ^{96}Ag populated by the β decay of the 16^+ isomer in ^{96}Cd [34], where the emission rate for $l = 2$ protons is expected to be at least 200 times greater than for $l = 4$ protons due to the centrifugal barrier. On the other hand, the emission of $l = 0$ protons from the $s_{1/2}$ orbital is suppressed due to its low spectroscopic factor is excluded from further study. Quadrupole deformation was assumed to be zero for ^{101}In, which is close to the doubly magic ^{100}Sn. The latest finite-range droplet model (FRDM) quotes the quadrupole deformation parameter β_2 of ^{101}In to be 0.032 [35]. Using this theoretical β_2 value instead can shift the proton emission branch $T_{1/2}$ up by 30%, which is a small effect compared to the $T_{1/2}$ variation caused by the uncertainty in S_p. An extrapolated value of S_p for ^{101}In at 1710(200) keV [30] was adopted in the half-life derivation, and all protons which are emitted from any excited state in ^{101}In are assumed to populate the ground state of ^{100}Cd. Even though 10(5)% of

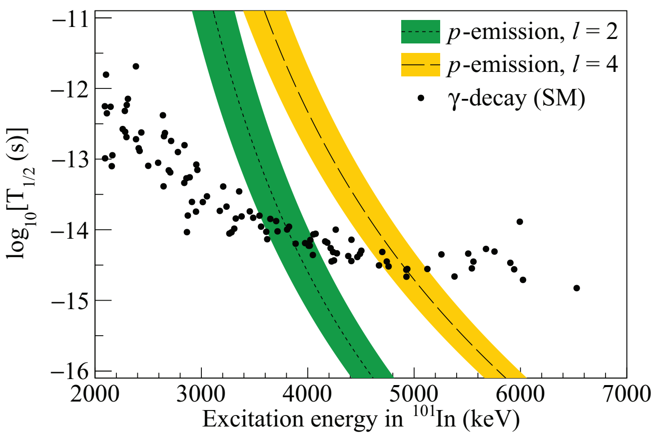

FIG. 7. Calculated partial half-lives of electromagnetic decay (points) and proton emission (lines and color bands) modes of predicted excited states in ^{101}In as a function of excitation energy. The proton emission half-life curves with $l = 2$ and $l = 4$ were derived based on Ref. [32] and $S_p = 1710(200)$ keV [30], where the colored bands correspond to the 1σ variations in S_p. The points are derived from SM calculations.

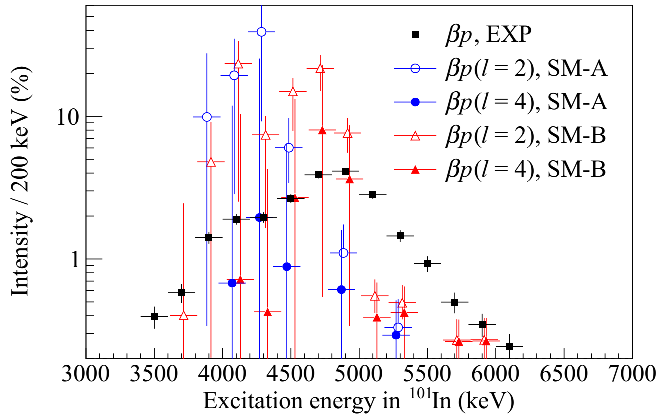

FIG. 8. Intensity distributions of β-delayed proton emission branches as a function of the excitation energy in ^{101}In. SM-A and SM-B refer to the assumed ground-state spins of ^{101}Sn being $5/2^+$ or $7/2^+$, respectively. The experimental $E_{\beta p}$ spectrum adopted from Ref. [23] was shifted by the proton separation energy of ^{101}In [30] and corrected for β-particle energy summing effects as discussed in Ref. [36]. See the text for details.

the overall $b_{\beta p}$ was measured to populate the 1004-keV 2_1^+ state in ^{100}Cd, in good agreement with 11(3)% from a previous measurement [16], all of the calculated βp emission branch was assumed to populate the ground state of ^{100}Cd for the sake of simplicity in this theoretical exercise. Partial half-lives of the γ-decaying states were extracted from NuShellX outputs. This approach was also applied to the decay of ^{99}In with $S_p(^{99}\mathrm{Cd}) = 4150(30)$ keV [30], and the predicted $b_{\beta p}$ value of ^{99}In is less than 0.1% regardless of the angular momentum of the emitted protons—somewhat lower but comparable to the experimental value of 0.29(3)%.

The decay partial half-life comparisons for excited states in ^{101}In with >0.01% feeding are shown in Fig. 7. Against the emission of $l = 2$ protons, γ-ray decay branches are expected to be dominant if $E_x < 3600$ keV and vice versa at $E_x > 4200$ keV. When protons are to be emitted with $l = 4$, the energy condition for sizable $b_{\beta p}$ values is $E_x > 5200$ keV—higher than with $l = 2$ due to the centrifugal barrier. Changes in partial half-lives of γ-ray transitions due to variations in effective charges and magnetic g-factors were less than 5%. All of the SM electromagnetic transition branches for ^{101}In were derived from the effective charge set $e_p/e_n = 1.5/1.4e$ and $g_s^{\mathrm{eff}} = 0.7g_s^{\mathrm{free}}$. This result was convoluted with theoretical b_β values from the SM to yield hypothetical βp energy spectra for the two hypotheses on the ground-state spin of ^{101}Sn, as shown in Fig. 8. The experimental βp energy spectrum was adjusted by the extrapolated S_p value and β-particle energy summing effects in the same DSSSD pixel where proton emission would occur [36]. The implantation depth of ^{101}Sn ions in WAS3ABi was assumed to be 500 μm, leading to an approximate energy correction of 170(140) keV. In this article, we denote the $J^\pi(^{101}\mathrm{Sn}) = 5/2^+$ and $J^\pi(^{101}\mathrm{Sn}) = 7/2^+$ hypotheses as SM-A and SM-B, respectively. The SR88MHJM interaction predicts $J^\pi(^{101}\mathrm{Sn}) = 5/2^+$, but the $7/2^+$ state is nearly degenerate with the ground state. The calculation of β-decay branches from this $7/2^+$ state could be carried out as if it were the ground state in NuShellX. Higher b_β values for states in ^{101}In with $E_x > 4400$ keV were calculated for SM-B compared to SM-A for both $l = 2$ and $l = 4$ protons. This result is consistent with the average E_x calculated in a systematics study of GT β decays in the ^{100}Sn region [12]. The βp emission branching ratio distributions as a function of the excitation energy in ^{101}In were compared with the experimental βp energy spectrum from Ref. [23], between the different angular momenta $l = 2$ and $l = 4$.

The expected βp intensity distributions assuming the emission of $l = 2$ protons become nearly identical with the β-decay distributions where $E_x > 4200$ keV, and consequently the $b_{\beta p}$ values are predicted to be >75% for both SM-A and SM-B. However, only a 1σ increase in the extrapolated S_p value of ^{101}In and 1σ-reduced b_β values can lower the unreasonably large $b_{\beta p}$ values down to 17% (SM-A) and 34% (SM-B), much closer to the experimental value of 23.6(8)%. When assuming the emission of only $l = 4$ protons, the double peak structure of the βp energy distribution calculated based on the $J^\pi(^{101}\mathrm{Sn}) = 7/2^+$ hypothesis (see Fig. 4 in Ref. [11]) is not observed with this approach due to heavy suppression of proton emission branches at $E_x < 4600$ keV. After summing the $b_{\beta p}$ values for each excited state populated by both β decays and γ-ray feeding, the cumulative theoretical $b_{\beta p}$ values for SM-A and SM-B were $4.8^{+45.4}_{-4.3}$% and $17.1^{+46.5}_{-15.4}$%, respectively. The large uncertainties, especially towards higher $b_{\beta p}$ values, are attributed to the large uncertainties on the S_p value of ^{101}In and b_β values for high-energy excited states.

All of the four predicted excitation energy spectra for βp emission are shifted towards lower values than the experimental intensities, because the predicted β-decay scheme fails to sufficiently populate excited states in ^{101}In with $E_x > 5000$ keV. A possible explanation is the model space truncation which did not permit the ground-state wave function of ^{101}Sn to include core excitation components above the

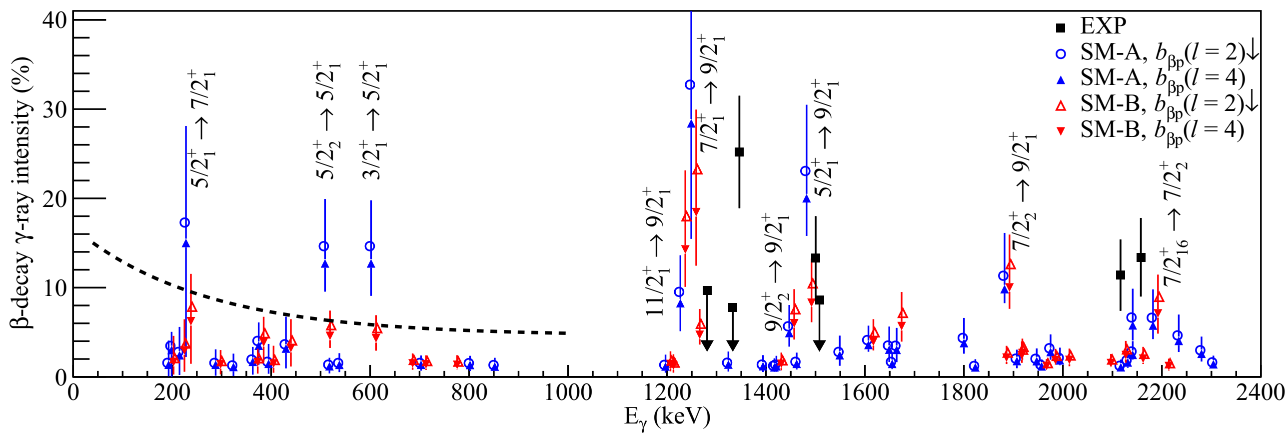

FIG. 9. Experimental (black) and theoretical (blue and red) β-delayed γ-ray intensities in ^{101}In. The discriptions of SM-A and SM-B are the same as in Fig. 8. The black points with arrows correspond to 2σ upper limits on the intensities of the γ rays which were previously reported but not observed in this work. The black dashed curve at $E_\gamma < 1000$ keV illustrates a 2σ upper limit on γ-ray intensities derived from statistical fluctuations in the energy spectrum displayed in Fig. 5. The initial-final spin labels are taken from SM calculations. For the sets with $l = 2$ proton emission, the downward arrows in the legend indicate the results obtained with reduced $b_{\beta p}$ values after raising the extrapolated S_p value by 1σ and adopting the 1σ-reduced b_β values for proton-emitting states.

$N = Z = 50$ shell closure. One should also consider the 7% extrapolated uncertainty on the excitation energies in ^{101}In from this SM, which can lead to shifts in β-decay intensity distributions by more than 500 keV at high-energy states. From these results, the ground-state spin assignment of ^{101}Sn from the overall $b_{\beta p}$ value and its distribution in energy remains ambiguous.

Theoretical γ-ray intensity distributions populated by the β decay of ^{101}Sn were derived from both SM-A and SM-B. Unlike the β decay of ^{99}In, non-negligible reductions in branching ratios due to proton emission at highly excited states were calculated by comparing the partial half-lives of proton/γ decay modes for each excited state. Since the experimental γ-ray intensities were normalized to the number of β decays minus the identified βp events, theoretical $b_{\beta p}$ values were also applied when normalizing the theoretical γ-ray intensities. The overestimated $l = 2$ proton emission branching ratios was moderated by the 1σ increase in the S_p value and 1σ reduction in the b_β values of ^{101}In. The γ-ray intensities calculated after this moderation were slightly higher but consistent within large uncertainties of the derived I_γ values assuming $l = 4$ proton emission.

The comparisons with the experimental γ-ray intensities are shown in Fig. 9. Similar to ^{99}Cd, the most intense γ ray at 1346 keV was well reproduced by both SM-A and SM-B, albeit the ≈100-keV energy difference. The predicted transition for this γ ray in ^{101}In is $7/2^+_1 \to 9/2^+_1$, but an alternative suggestion of $11/2^+_1 \to 9/2^+_1$ from SM-B with a non-negligible intensity and slightly lower γ-ray energy cannot be rejected. The intensity of the 1500-keV γ ray was also well reproduced by both models, and its experimental uncertainty allows two possible initial spin assignments: $5/2^+_1$ or $9/2^+_2$. The calculations offered two candidates with sufficient intensities for the two newly observed γ rays above 2000 keV: one from a highly excited state with $E_x = 4074$ keV with $E_\gamma = 2187$ keV to the $7/2^+_2$ state, and a γ ray from the $7/2^+_2$ state to the ground state. The theoretical energy of the $7/2^+_2 \to 9/2^+_1$ transition is 1887 keV, slightly lower than either of the 2116- or 2157-keV experimental energies but in a reasonable agreement. The predicted branching ratio of the 4074-keV state to the $7/2^+_2$ state is 40(6)%, and no other γ-ray from this state has a branching ratio greater than 8%. On the other hand, the calculated branching ratio of the $7/2^+_2$ state to the ground state is 64(10)%, which is greater than the only other significant branching ratio of 20(3)% to the $9/2^+_2$ state at 1452 keV. Given higher statistics, it would be of interest to check whether the two high-energy γ rays are indeed in coincidence. The most significant discrepancy between SM-A and SM-B was found in the $E_\gamma < 1000$ keV region, where three γ rays depopulating $3/2^+_1$ and $5/2^+_{1,2}$ states with energies of approximately 200, 500, and 600 keV are predicted with $I_\gamma > 12\%$ for SM-A and $I_\gamma < 6\%$ for SM-B. Experimentally, these low-energy γ rays were not observed. Instead, a 2σ upper limit curve on the intensity of hypothetical γ-ray candidates with energies below 1000 keV was derived based on the statistical fluctuations shown in Fig. 5 and corrected for the EURICA efficiency. The curve rises at lower energies mainly because of the accumulation of Compton background spectra from every γ ray. This curve lies below the expected intensities of the three low-energy γ rays from SM-A, but the aforementioned limitations of the SM regarding core excitations can introduce further variations $B(M1)$ and $B(E2)$ values which would increase the uncertainties of the predicted I_γ values. One criticism against the SM-B result in the γ-ray intensity evaluation is the large I_γ prediction for the $11/2_1 \to 9/2^+_1$ transition, and this hypothesis can be tested by searching for a γ ray with a similar energy as the 1346 keV transition.

A summary of the assignment of the γ rays in ^{101}In is presented in Fig. 10. The assignment of the two high-energy γ rays is highly tentative. The two confirmed γ rays at 1346 and 1500 keV were placed in the level scheme of ^{101}In, but the spins of the two excited states were left with alternative

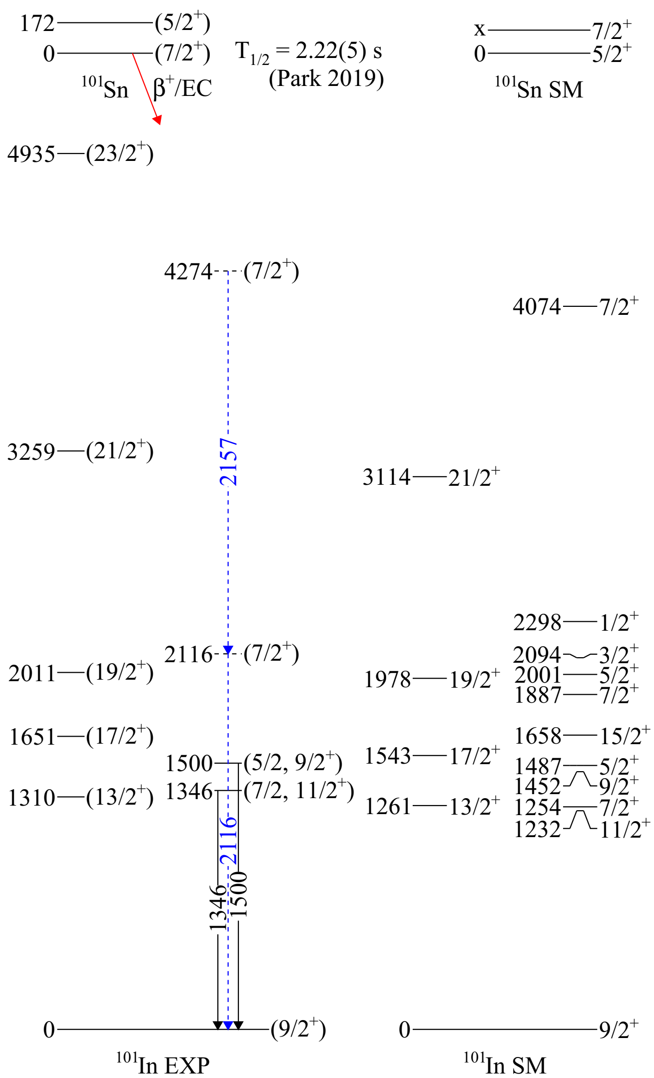

FIG. 10. Level schemes of ^{101}In from the $\beta\gamma$ spectroscopy of ^{101}Sn. The half-life of ^{101}Sn was determined in a previous work (Park 2019 [23]). The transitions and the level energies are in keV. The theoretical excitation energy of the $7/2^+$ state in ^{101}Sn is within $\approx$100 keV of the $5/2^+$ state. In ^{101}In, the excited states above the label "FE EXP" were previously assigned in a fusion-evaporation experiment [8] and not populated in this experiment. For the SM results, only the states which are most relevant for the comparison are presented. The SM states without J^π labels have the same values as the adjacent experimental states. The assignment of the 2116- and 2157-keV γ rays observed in this work is very tentative, as indicated with blue dashed lines. See the text for discussion.

suggestions. The high-spin states which were first uncovered in Ref. [8] were well reproduced in energy by the SR88MHJM interaction, and additional low-spin states may be revealed with more statistics and a more efficient γ-ray spectroscopy setup. Besides the observed γ rays, both SM-A and SM-B predict γ-ray intensities $\leqslant 5\%$ for all other transitions and offer a reasonable explanation for the statistical challenges and discrepancies in literature concerning the $\beta\gamma$ spectroscopy results on ^{101}Sn.

V. CONCLUSION AND OUTLOOK

New results were obtained from the β-delayed γ-ray spectroscopy of ^{99}In and ^{101}Sn, both of which are one nucleon away from the doubly magic ^{100}Sn. In this work, SM calculation outputs on allowed GT β-decay branches and prompt $M1$, $E2$ γ-ray decay schemes were combined in order to perform a direct comparison with the experimental $\beta\gamma$ intensities and coincidence relationships in the daughter nuclei ^{99}Cd and ^{101}In. Theoretical uncertainties were derived based on small perturbations on the energies of excited states and cascading γ-ray transitions. A good agreement on the measured energies and intensities of the dominant γ-ray transitions was achieved with this method, but certain ambiguities on both the theoretical and experimental sides remained.

The level scheme of ^{99}Cd was supplemented by many tentative, new γ rays which are probably associated with low-spin excited states, populated by the β decay of the $(9/2^+)$ ground state of ^{99}In. Several new states with tentative spin-parity assignments were proposed based on the close agreement between the experimental and theoretical results on γ-ray energies, intensities, and coincidence relationships. A more comprehensive data set on high-multiplicity $\gamma\gamma$ coincidences and angular correlations will enable more robust assignments of the observed γ rays and spins of excited states which are formed by a neutron above the $N = 50$ shell and a proton hole pair below the $Z = 50$ shell.

The structure and β decay of ^{101}Sn were assessed in the framework of SM calculations, and were complemented by a semiempirical proton emission theory in order to reproduce the experimental βp energy spectrum and the overall $b_{\beta p}$ value. In order to reproduce the experimental $B_{\rm GT}$, $T_{1/2}$ values and βp energy spectra, theoretical efforts on the structure and decay of ^{101}Sn should include core excitation and an expanded model space. Both the βp emission branching ratios and the β-decay γ-ray intensities were discussed in the context of the ground-state spin of ^{101}Sn, without a convincing evidence for either the $5/2^+$ or the $7/2^+$ assignment. Improvements in the mass measurements of ^{101}Sn, ^{101}In and ^{100}Cd, as well as significantly improved statistics for β-delayed γ rays of ^{101}Sn may address this question and its consequence on the evolution of the neutron $g_{7/2}$ orbital relative to the $d_{5/2}$ orbital above the $N = 50$ shell closure along the tin isotopic chain.

ACKNOWLEDGMENTS

The authors would like to thank the personnel at the RIKEN Nishina Center for providing the exotic radioactive isotope beam with record intensities. This experiment was performed at RI Beam Factory operated by RIKEN Nishina Center and CNS, University of Tokyo. We acknowledge the EUROBALL Owners Committee for loaning the germanium detectors and the PreSpec Collaboration for the readout electronics of the cluster detectors of EURICA. Support for the WAS3ABi setup was provided by the Rare Isotope Science Project, funded by the Ministry of Education, Science and Technology (MEST) and National Research Foundation (NRF) of Korea, as well as KAKENHI

(Grant No. 25247045) of Japan Society for the Promotion of Science (JSPS). This work was supported by the Institute for Basic Science (IBS-R031-D1). The authors acknowledge also the support of the DFG cluster of excellence "Origin and Structure of the Universe," German BMBF under Contracts No. 05P15PKFNA and No. 05P19PKFNA, and the Spanish Ministerio de Economía y Competitividad via Project No. FPA2017-84756-C4-2-P. Part of the research was funded by the Natural Sciences and Engineering Research Council (NSERC) of Canada and also supported by FJNSP LIA (French-Japanese International Associated Laboratory for Nuclear Structure Problems).

[1] A. Gade and T. Glasmacher, Prog. Part. Nucl. Phys. **60**, 161 (2008).
[2] O. Sorlin and M.-G. Porquet, Prog. Part. Nucl. Phys. **61**, 602 (2008).
[3] R. Kanungo *et al.*, Phys. Rev. Lett. **102**, 152501 (2009).
[4] D. Steppenbeck *et al.*, Nature (London) **502**, 207 (2013).
[5] T. Otsuka, T. Suzuki, R. Fujimoto, H. Grawe, and Y. Akaishi, Phys. Rev. Lett. **95**, 232502 (2005).
[6] T. Otsuka, T. Suzuki, M. Honma, Y. Utsuno, N. Tsunoda, K. Tsukiyama, and M. Hjorth-Jensen, Phys. Rev. Lett. **104**, 012501 (2010).
[7] H. Grawe *et al.*, Nucl. Phys. A **704**, 211c (2002).
[8] M. Lipoglavšek *et al.*, Phys. Rev. C **66**, 011302(R) (2002).
[9] M. Lipoglavšek *et al.*, Phys. Rev. Lett **76**, 888 (1996).
[10] D. Seweryniak *et al.*, Phys. Rev. Lett. **99**, 022504 (2007).
[11] O. Kavatsyuk *et al.*, Eur. Phys. J. A **31**, 319 (2007).
[12] L. Batist *et al.*, Eur. Phys. J. A **46**, 45 (2010).
[13] I. G. Darby *et al.*, Phys. Rev. Lett. **105**, 162502 (2010).
[14] T. D. Morris *et al.*, Phys. Rev. Lett. **120**, 152503 (2018).
[15] T. Faestermann, M. Górska, and H. Grawe, Prog. Part. Nucl. Phys. **69**, 85 (2013).
[16] K. Straub, Ph.D. thesis, Technische Universität München, 2010 (unpublished).
[17] N. Fukuda *et al.*, Nucl. Instrum. Methods B **317**, 323 (2013).
[18] T. Kubo *et al.*, Prog. Theor. Exp. Phys. **2012**, 03C003 (2012).
[19] S. Nishimura, Prog. Theor. Exp. Phys. **2012**, 03C006 (2012).
[20] P.-A. Söderström *et al.*, Nucl. Instrum. Methods B **317**, 649 (2013).
[21] J. Park *et al.*, Phys. Rev. C **96**, 044311 (2017).
[22] J. Park *et al.*, Phys. Rev. C **97**, 051301(R) (2018).
[23] J. Park *et al.*, Phys. Rev. C **99**, 034313 (2019).
[24] D. Lubos *et al.*, Phys. Rev. Lett. **122**, 222502 (2019).
[25] G. Audi *et al.*, Chin. Phys. C **41**, 030001 (2017).
[26] T. Kibédi *et al.*, Nucl. Instrum. Methods A **589**, 202 (2008).
[27] Evaluated Nuclear Structure Data File (ENSDF), http://www.nndc.bnl.gov/ensdf/.
[28] D. T. Yordanov *et al.*, Phys. Rev. C **98**, 011303(R) (2018).
[29] B. A. Brown and W. D. M. Rae, Nucl. Data Sheets **120**, 115 (2014).
[30] M. Wang *et al.*, Chin. Phys. C **41**, 030003 (2017).
[31] B. J. Coombes *et al.*, Phys. Rev. C **100**, 024322 (2019).
[32] D. S. Delion, R. J. Liotta, and R. Wyss, Phys. Rep. **424**, 113 (2006).
[33] I. Čeliković *et al.*, Phys. Rev. Lett. **116**, 162501 (2016).
[34] P. J. Davies *et al.*, Phys. Lett. B **767**, 474 (2017).
[35] P. Möller, A. J. Sierk, T. Ichikawa, and H. Sagawa, At. Data Nucl. Data Tables **109–110**, 1 (2016).
[36] Z. Meisel *et al.*, Nucl. Instrum. Methods A **844**, 45 (2017).